Parasitol Res (2002) 88: 198–207
DOI 10.1007/s00436-001-0527-x

ORIGINAL PAPER

P. Alvarez-Pellitero · K. Molnár · A. Sitjà-Bobadilla
C. Székely

Comparative ultrastructure of the actinosporean stages of *Myxobolus bramae* and *M. pseudodispar* (Myxozoa)

Received: 27 July 2001 / Accepted: 13 September 2001 / Published online: 9 November 2001

Abstract The ultrastructrure of triactinospores and other developmental stages obtained after the experimental infection of the oligochaete *Tubifex tubifex* with myxospores of *Myxobolus bramae* and *Myxobolus pseudodispar* was studied. In both cases, pansporocysts harbouring spores and the remnants of polar bodies were found in the gut epithelium of the tubificids. Other stages were also seen in *M. pseudodispar*. Capsulogenic cells surrounded the apical part of the sporoplasm in *M. bramae* whereas they were located separately in *M. pseudodispar*. The sporoplasm of *M. bramae* was elongated and was filled with numerous infective cells, whereas secondary cells rarely appeared in the sporoplasm of *M. pseudodispar*, which contained large groups of *β*-glycogen granules. Other *M. pseudodispar* stages included pansporocysts harbouring pregametic or gametic stages, zygotes, or the initial steps of sporogenesis. The presence of first- and second-order polar bodies indicates the existence of meiosis. In the spores of *M. pseudodispar*, the presence of desmosome-like junctions between the capsulogenic cells, and hemidesmosome-like junctions between the capsulogenic cells and the inner membrane of the valvogenic cells, is remarkable.

Introduction

Since Wolf and Markiw (1984) experimentally proved that *Triactinomyxon gyrosalmo,* previously included in the class Actinosporea, was actually a stage of *Myxobolus cerebralis* developing in an oligochaete alternate host, the research on myxosporean parasites has become a focus of interest. Numerous works have been published on the development, systematics and anatomical structure of various myxosporean species. Until now, the actinospore stage of more than 20 myxosporean species has been identified (see Molnár et al. 1999), and new data have also been obtained on the ultrastructure of actinosporeans. Prior to the start of this experimental work, only De Puytorac (1963), Ormieres (1970) and Marques (1982, 1983, 1984, 1986) had studied the ultrastructure of actinosporeans. As the developmental cycles gradually became known, however, research in this field became more intensive. Knowledge of the life cycles also allowed the development of experimental infections which provided adequate material for different studies including those on ultrastructure. In the last decade, Lom and Dyková (1992, 1997), Grossheider (1994), Koller (1994), and Lom and Dyková (1997) provided detailed data on the ultrastructure of some actinospores. Apart from a few remarks made by the above authors on some early intraoligochaete developmental stages, detailed data on the ultrastructure of early actinosporean developmental stages came mainly from the studies performed by El-Matbouli and Hoffmann (1998) on *M. cerebralis*.

This paper presents data on the ultrastructure of triactinospores and developmental stages obtained after the experimental infections of the oligochaete *Tubifex tubifex* Müller with myxospores of *Myxobolus bramae* Reuss, 1906 and *Myxobolus pseudodispar* Gorbunova, 1936 parasites of the cyprinid fish *Abramis brama* (L.) and *Rutilus rutilus* L., respectively.

Materials and methods

Spores of *M. bramae* and *M. pseudodispar* were obtained from their fish hosts and used for experimental infections of the oligochaete *T. tubifex*, as described by Székely et al. (1999) and Eszterbauer et al. (2000), respectively. The infection of *T. tubifex* specimens was

P. Alvarez-Pellitero (✉) · A. Sitjà-Bobadilla
Instituto de Acuicultura de Torre de la Sal,
C.S.I.C., Ribera de Cabanes, 12595 Castellón, Spain
E-mail: alvarezp@iats.csic.es
Tel.: +34-96-4319500
Fax: +34-96-4319509

C. Székely · K. Molnár
Veterinary Medical Research Institute,
P.O. Box 18, Hungarian Academy of Sciences,
1581 Budapest, Hungary

checked according to the method developed by Yokoyama et al. (1991), using the examination of spore release from oligochaete specimens placed into cell-well plates. The intensity of infection of live oligochaetes releasing actinospores was studied by examining the oligochaetes under a coverslip by light microscopy at a magnification of 100–200×. The four specimens of *T. tubifex* showing the highest infection intensity by the actinospores of *M. bramae* or *M. pseudodispar* were selected and processed for transmission electron microscopy (TEM). They were cut into small pieces and fixed in 2.5% (v/v) glutaraldehyde in 0.1 M cacodylate buffer (pH 7.2), for 1 h at 4°C. Samples were washed several times with the same buffer, post-fixed in 1% (w/v) cacodylic OsO_4, dehydrated through a graded ethanol series, and embedded in Spurr's resin (Spurr 1969). Ultrathin sections were double-stained with uranyl acetate and lead citrate (Reynolds 1963). The sections were studied in Philips CM-10 and Hitachi H-800 transmission electron microscopes operating at 75–100 kV.

Results

Myxobolus bramae

Pansporocysts containing spores were found in the gut epithelium of the tubificid (Fig. 1). Up to six of the eight actinospores, sectioned at different levels, could be counted in the sections. Most of the space within the

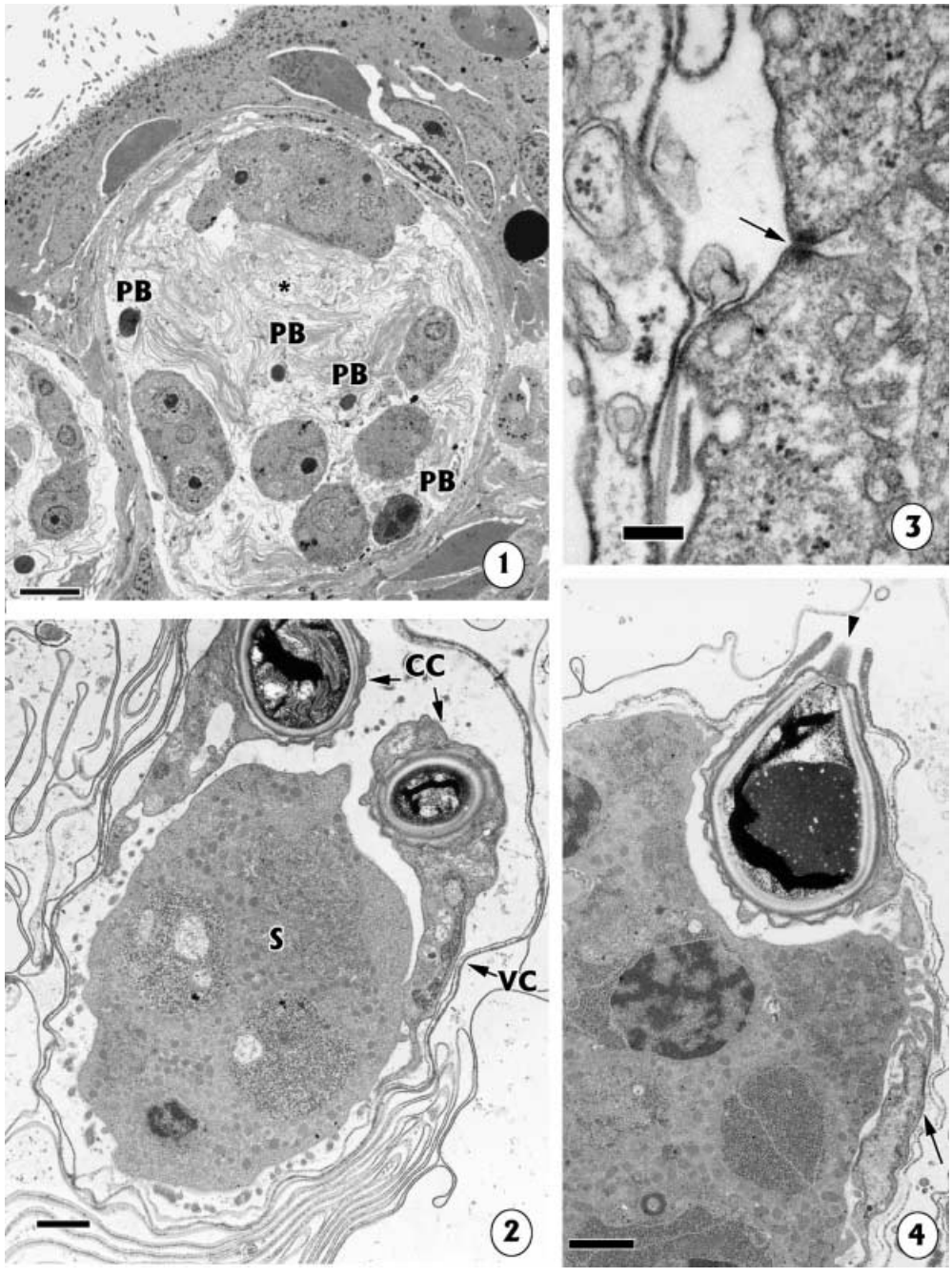

Figs. 1–4 Transmission electron micrographs of *Myxobolus bramae* actinosporean stages in the tubificid host

Fig. 1 Panoramic view of pansporocysts harbouring spores sectioned at the sporoplasm level in the gut epithelium. Notice the telescopically folded membranes of the style and the caudal extensions of the spores (*). *PB* Polar bodies. *Bar* 5 μm

Fig. 2 Oblique section of the apical part of a spore showing the two capsulogenic cells (*CC*), the apical part of the sporoplasm (*S*) and valvogenic cells (*VC*). Notice the location of CC as lateral shields of *S*. *Bar* 1 μm

Fig. 3 Detail of the junction between two enveloping cells of the pansporocyst. *Bar* 0.2 μm

Fig. 4 Longitudinal section of a spore showing a polar capsule and the apical part of the sporoplasm. A flattened portion of a capsulogenic cell can be observed laterally to the sporoplasm (*arrow*). Notice the hiatus of the valves and the plug in the apical part of the polar capsule (*arrowhead*). *Bar* 1 μm

pansporocyst was occupied by the telescopically folded doublets of the membranes of valvogenic cells forming the styles and caudal extensions of the spores (Figs. 1, 2). Sporoplasms and valvogenic cells of the spores were located among these membranes. Remnants of the polar bodies were also observed (Fig. 1). The somatic cells of the pansporocysts appeared flattened, with few organules in the cytoplasm and a flattened nucleus (when visible) (Fig. 1). They were connected by electron-dense cell junctions, reminiscent of tight junctions (Fig. 3).

Each spore was enveloped by three valvogenic cells. In most of the observed spores, the valvogenic cells were reduced to very thin, 100–120 nm, membrane doublets (Figs. 2, 4). These parts of the valvogenic cells were made up of two electron-dense membranes and an electron-lucent inner part. The valvogenic cell doublets loosely enveloped the capsulogenic cells and the sporoplasm, leaving a relatively large space between them. No cell junctions could be observed between the valvogenic membrane doublets and the capsulogenic cells or the membrane doublets and the sporoplasm. However, a membrane-free hiatus was left at the place of filament extrusion of the polar capsules (Fig. 4). The caudal part of the valvogenic cells, which constituted the style and the caudal extensions of the spores, was exclusively composed of the telescopically folded doublets of the valvogenic membranes (Fig. 2).

Figs. 5–7 Transmission electron micrographs of triactinospores of *Myxobolus bramae*

Fig. 5 Oblique section of a spore showing the three capsulogenic cells and the sporoplasm (*S*) extruding among them. Notice the electron-lucent space surrounding the polar capsule wall (*arrow*). *Bar* 1 μm

Fig. 6 Detail of the apical part of the polar capsule in Fig. 5 showing the longitudinal ribs of the wall (*arrow*). *Bar* 0.5 μm

Fig. 7 Cross-section of a sporoplasm with several secondary cells. Parts of the capsulogenic cells surround the sporoplasm even at this level. Notice the sinuous connections between contiguous capsulogenic cells (*arrow*) and the valve sutures (*arrowheads*). *Bar* 2 μm. *Inset* Detail of a capsulogenic cell connection (*arrow*) and a valve suture. *Bar* 0.5 μm

Capsulogenic cells were located at the apical end of the spore. The three capsulogenic cells surrounded the apical part of the sporoplasm, which extruded among them (Fig. 2). The cytoplasm of the capsulogenic cells contained vacuoles, some mitochondria with scarce cristae and glycogen granules (Figs. 2, 5). The nucleus was located in the basal part of the cell.

The wall of the polar capsule was surrounded by an electron-lucent space delimited from the cytoplasm of the capsulogenic cell by a dense envelope (Fig. 5). The wall of the polar capsule was composed of an outer electron-dense layer and a thicker electron-lucent inner layer inside which the polar filament formed helically arranged coils (Fig. 5). The end of the opening of the polar capsule was closed by a cap-like plug, which appeared to be in direct contact with the outspore space through a gap in the valvogenic membrane doublets (Fig. 4). The ribs of the capsule wall were observed in some sections (Fig. 6).

The sporoplasm was elongated and consisted of a primary cell which was filled with numerous infective, secondary cells (Figs. 7, 8) It showed pseudopodia-like projections which were less abundant in more advanced sporoplasms. A remnant of a vegetative nucleus was observed in some sections (Fig. 8). The association of a nucleus with each infective cell was not observed. The

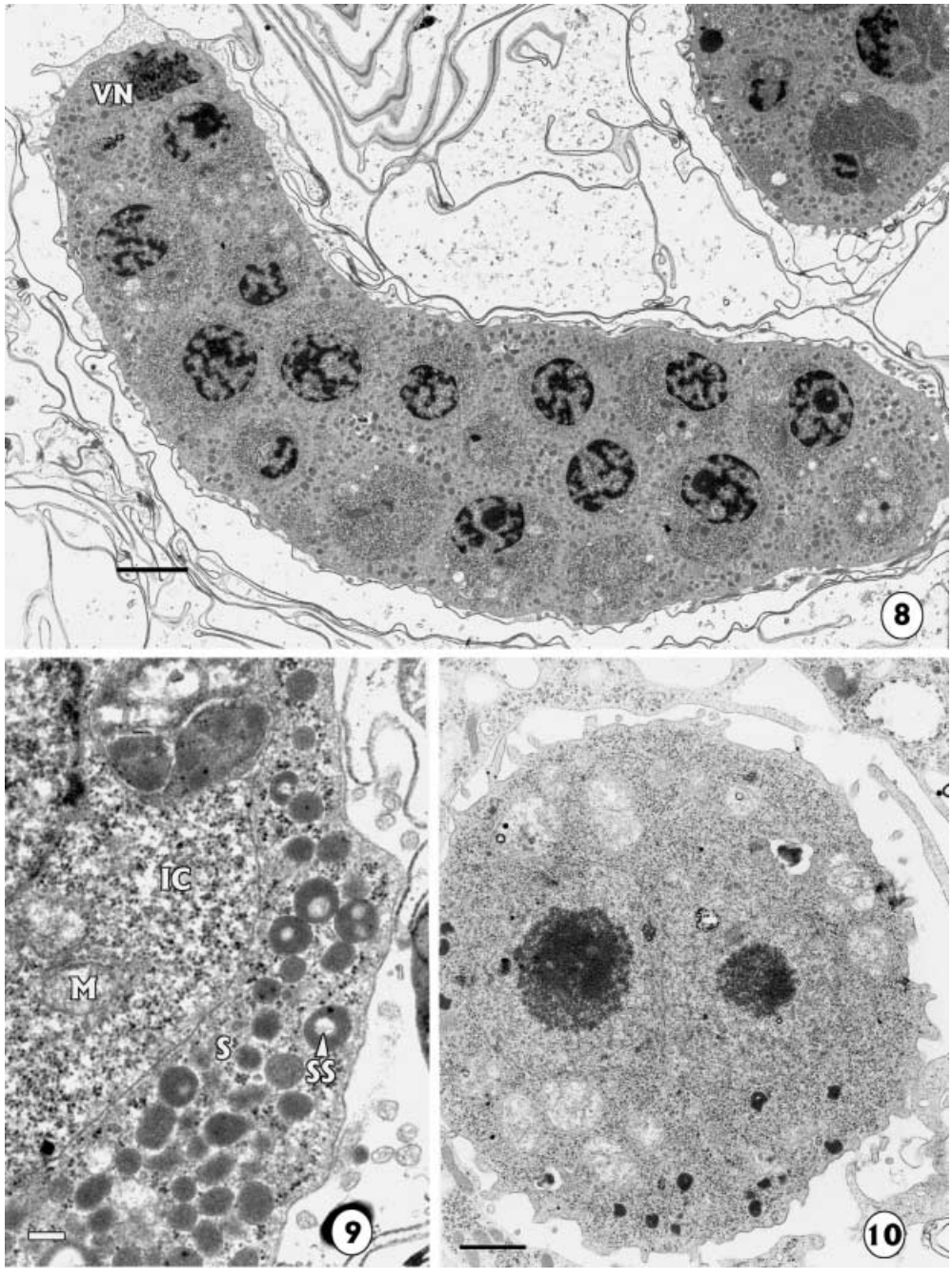

Figs. 8–10 Transmission electron micrographs of triactinospores of *Myxobolus bramae*

Fig. 8 Longitudinal section of a sporoplasm with numerous secondary cells and a vegetative nucleus (*VN*). Notice the small pseudopodia in the sporoplasm and the thin valvogenic membrane. *Bar* 2 μm

Fig. 9 Detail of a sporoplasm (*S*) with an infective cell (*IC*). *M* Mitochondria, *SS* sporoplasmosomes. *Bar* 0.2 μm

Fig. 10 Section of a sporoplasm with two recently divided nuclei. *Bar* 1 μm

cytoplasm of the primary cell had a scarcely granulated matrix and contained abundant electron-dense granules, some vacuoles and small, roundish sporoplasmosomes, sometimes with a lighter inner core (Fig. 9). Secondary cells were uninucleated, with the cytoplasm enveloped by a thin membrane, densely packed with ribosomes and containing mitochondria and fine glycogen granules (Fig. 9). Its nucleus showed abundant heterochromatin and, on some occasions, a distinct, round and compact nucleolus could be observed.

The initial steps in the development of the sporoplasm appeared in some sections, showing two nuclei with scarcely visible nuclear membranes. The cytoplasm had ribosomes, some electron-dense granules and some mitochondria with few flattened cristae (Fig. 10).

Myxobolus pseudodispar

Pansporocysts at different developmental stages could be observed in the gut epithelium of the host, most of them harbouring spores (Fig. 11). As in the case of *M. bramae,* pansporocysts containing spores sectioned at different levels showed multiple convoluted membranes of the valvogenic cells constituting the styles and caudal extensions of the spores. Among these

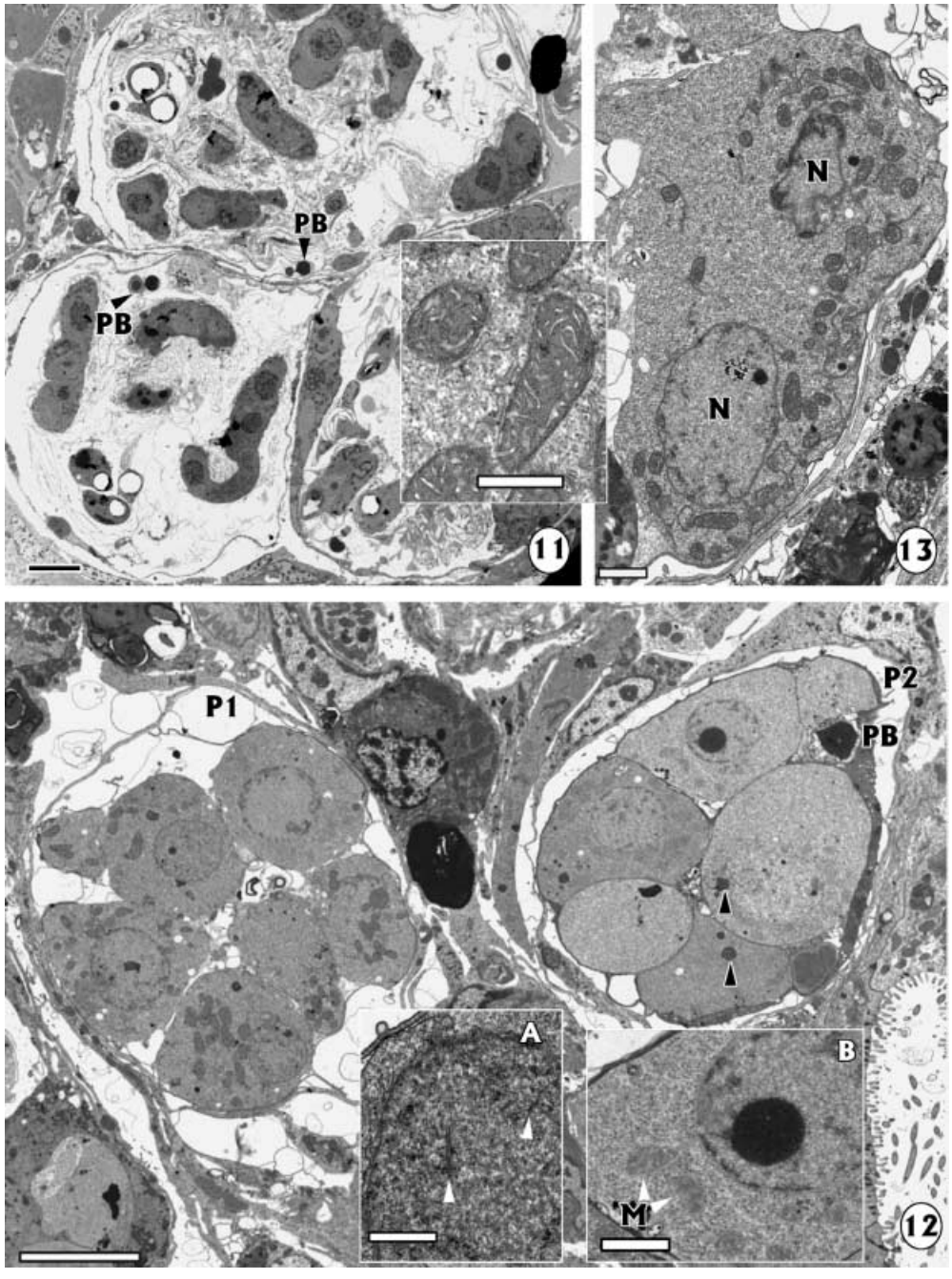

Figs. 11–13 Transmission electron micrographs of *Myxobolus pseudodispar* actinosporean stages in the tubificid host

Fig. 11 Panoramic view of several pansporocysts harbouring spores sectioned at different levels and some polar bodies (*PB*). *Bar* 5 μm

Fig. 12 Pansporocysts with pregametic (*P1*, left) and gametic (*P2*, right) stages in the gut epithelium. Notice the PB remnants of meiosis and the nucleoli remnants (*arrowheads*) in P2. *Bar* 5 μm. *Inset A* Detail of a nucleus of a pregametic cell showing microtubuli (*arrowheads*). *Bar* 0.5 μm. *Inset B* Detail of a gametic cell showing scarce mitochondria (*M*) and the nucleus with a nucleolus. *Bar* 1 μm

Fig. 13 Pregametic cell with two nuclei (*N*), abundant mitochondria and zig-zagging endoplasmic reticulum. *Bar* 1 μm. *Inset* Detail of mitochondria. *Bar* 0.5 μm

telescopically folded extensions of the shell valves, capsulogenic and sporoplasmic cells were located loosely in the pansporocyst. In some sections, remnants of the polar bodies could also be seen (Fig. 11).

Some of the stages prior to sporogenesis were also found in the intestinal epithelium. The youngest stage was a pansporocyst harbouring some inner cells (a maximum of six cells was observed in the sections), apparently at a pregametic stage, although it was difficult to differentiate α and β cells (Fig. 12). These inner cells showed nuclei with little heterochromatin and some microtubuli (Fig. 12, inset A), and cytoplasm with a homogeneous matrix containing mitochondria with well-developed flattened cristae, some ribosomes and endoplasmic reticulum. Binucleated α or β cells with abundant mitochondria and zig-zagging endoplasmic reticulum were sometimes observed (Fig. 13). Some pansporocysts harboured cells from the start of gametogenesis or soon after gamete formation, as some polar bodies, probably of first order, were also visible (Fig. 12). These cells were poorly electron-dense and had few organelles. Nucleoli were evident in the nuclei of some cells (Fig. 12, inset B), but other cells showed a dark mass, intracytoplasmatically located, which could have been a nucleolus remnant (Fig. 12). No clear synaptonemic complexes could be observed.

In more advanced stages, some cells resulting from the division of a zygote were detected (Fig. 14). In other pansporocysts, different steps of sporogony could be observed, as well as the asynchronous development of different spores and the presence of polar bodies, probably of the second order (Figs. 15, 16, 17). Valvogenic cells were visible, as well as capsulogenic cells arranged in the typical group of three closed cells (Fig. 15) and sporoplasmic cells containing infective cells (Fig. 16). In other sections, more advanced stages of the valvogenic cells surrounding probable capsulogenic and sporoplasmic cells were observed inside a pansporocyst (Fig. 17).

Somatic enveloping cells of the pansporocysts appeared flattened, with little cytoplasm (Figs. 12, 15, 17) and were connected by slightly electron-dense cell junctions (Fig. 17, inset). In pansporocysts containing more advanced sporogonic stages, the somatic cells were reduced to a thin membrane-like envelope which was thickened only in those parts where nuclei were located (Fig. 11).

Different steps of the development of the valvogenic cells could be observed (Figs. 15, 17). In sections obtained at a certain level, valvogenic cells showed the nucleus and the membrane folds of the styles starting to be formed (Fig. 18). Electron-dense junctions, resembling tight junctions, between adjacent valvogenic cells and between valvogenic and sporoplasmic cells could also be detected in such immature stages (Figs. 18, 19). Each mature spore was enveloped by three valvogenic cells which were united by sutures running along the axis of the spore. Cell junctions in the form of sutures appearing as simple adherent, aseptate junctions were

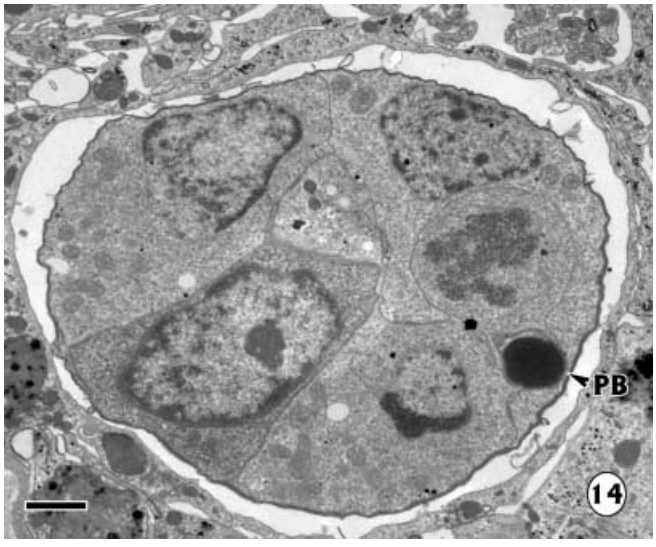

Fig. 14 Transmission electron micrograph of a *Myxobolus pseudodispar* actinosporean stage in the tubificid host. Pansporocyst harbouring a stage with several cells, probably resulting from zygote division. *PB* Polar body. *Bar* 1 μm

easily detectable at the apical end of the spores and in cross-sections at the level of the capsulogenic cell nucleus (Fig. 20). In mature spores, the valvogenic cells were reduced to a very thin, 75–80 nm, membrane doublet on most parts of the spore (Fig. 20). This part of the valvogenic cell was made up of two electron-dense membranes including an electron-lucent inner part. In some segments around the spore body, however, the intermediate part between the electron-dense sheets became enlarged and contained foamy cytoplasm (Fig. 20). The caudal part of the valvogenic cells, which constituted the style and the caudal extensions of the spores, was exclusively composed of telescopically folded doublets of the valvogenic membrane (Figs. 11, 20). Valvogenic cells only loosely covered the capsulogenic cells and the sporoplasm, leaving a large space between them.

The three elongated capsulogenic cells (Figs. 20, 21, 22) were closely attached to each other and well separated from the sporoplasm. The nuclei of the capsulogenic cells, with abundant heterochromatin, were found in the basal part of the cells. The cytoplasm harboured mitochondria with abundant tubular cristae and polysaccharide reserves (Fig. 22). The wall of the polar capsule was surrounded by an electron-opaque space which was delimited from the cytoplasm of the capsulogenic cell by a membrane (Fig. 21, 23). The wall of the polar capsule was composed of an electron-dense outer layer and a thicker electron-lucent inner layer. Inside these layers the polar filament formed helically arranged coils (Figs. 20, 21). At the apical end of the polar capsules, small spine-like formations were seen which corresponded to the surface ribs of the capsular wall (Fig. 23). Here, the opening of the polar capsule was closed by a cap-like

plug, which was in direct contact with the outspore space through a gap of the valvogenic membrane doublets (Fig. 23). Close to their apical ends, capsulogenic cells were connected by well-demonstrable desmosome-like cell junctions, whereas junctions of the hemidesmosomal type connected the apical surface of the capsulogenic cells to the inner membrane of the valvogenic cell (Fig. 24).

Different steps of sporoplasm division were observed. In what was probably an initial stage, a vegetative nucleus appeared beside the very dark, condensed nucleus of an infective cell which was not yet surrounded by a membrane (Fig. 25). In other sections, several infective, secondary cells appeared inside the sporoplasm, apparently at different stages of development, some of which had well-developed mitochondria. The nucleus could appear either very condensed or with little heterochromatin (Fig. 26). Other sporoplasms contained mature secondary cells sectioned at different levels (Fig. 27). In the course of maturation, the cytoplasm of the sporoplasmic cell became progressively darker and filled with electron-dense inclusions and a few sporoplasmosomes. Large groups of β-glycogen granules were also seen (Figs. 27, 28), as well as a few mitochondria. The infective, secondary cells had a chromatin-rich nucleus (a small nucleolus was sometimes visible) and

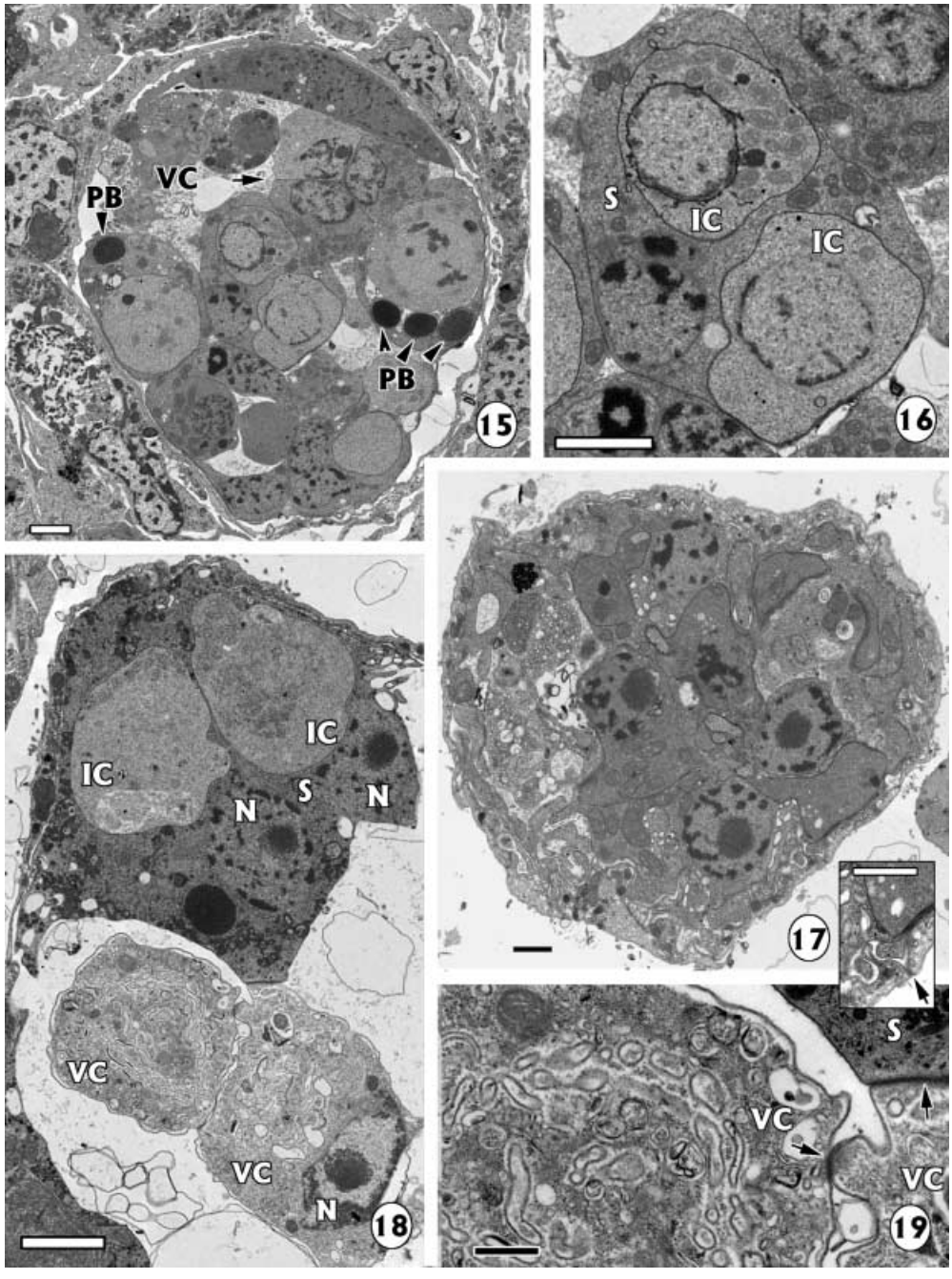

Figs. 15–19 Transmission electron micrographs of *Myxobolus pseudodispar* actinosporean stages in the tubificid host

Fig. 15 Pansporocyst harbouring different stages of spore development. Notice the three capsulogenic cells transversally sectioned (*arrow*), a valvogenic cell (*VC*) and polar bodies (*PB*). *Bar* 2 μm

Fig. 16 Detail of the central cell in Fig. 15, a probable initial sporoplasm (*S*) with one vegetative nucleus and two infective cells (*IC*). *Bar* 2 μm

Fig. 17 Pansporocyst formed by several cells connected by junctions (*inset*, *arrow*), harbouring valvogenic cells and differentiating capsulogenic and sporoplasmic cells. *Bars* 1 μm

Fig. 18 Part of a pansporocyst showing a sporoplasm (*S*) with two infective cells (*IC*) and two nuclei (*N*), and the caudal part of two valvogenic cells (*VC*). Notice the abundant membranes of the forming styles and the nucleus (*N*). *Bar* 2 μm

Fig. 19 Details of the junctions between S and VC and between both VC appearing in Fig. 18. *Bar* 0.5 μm

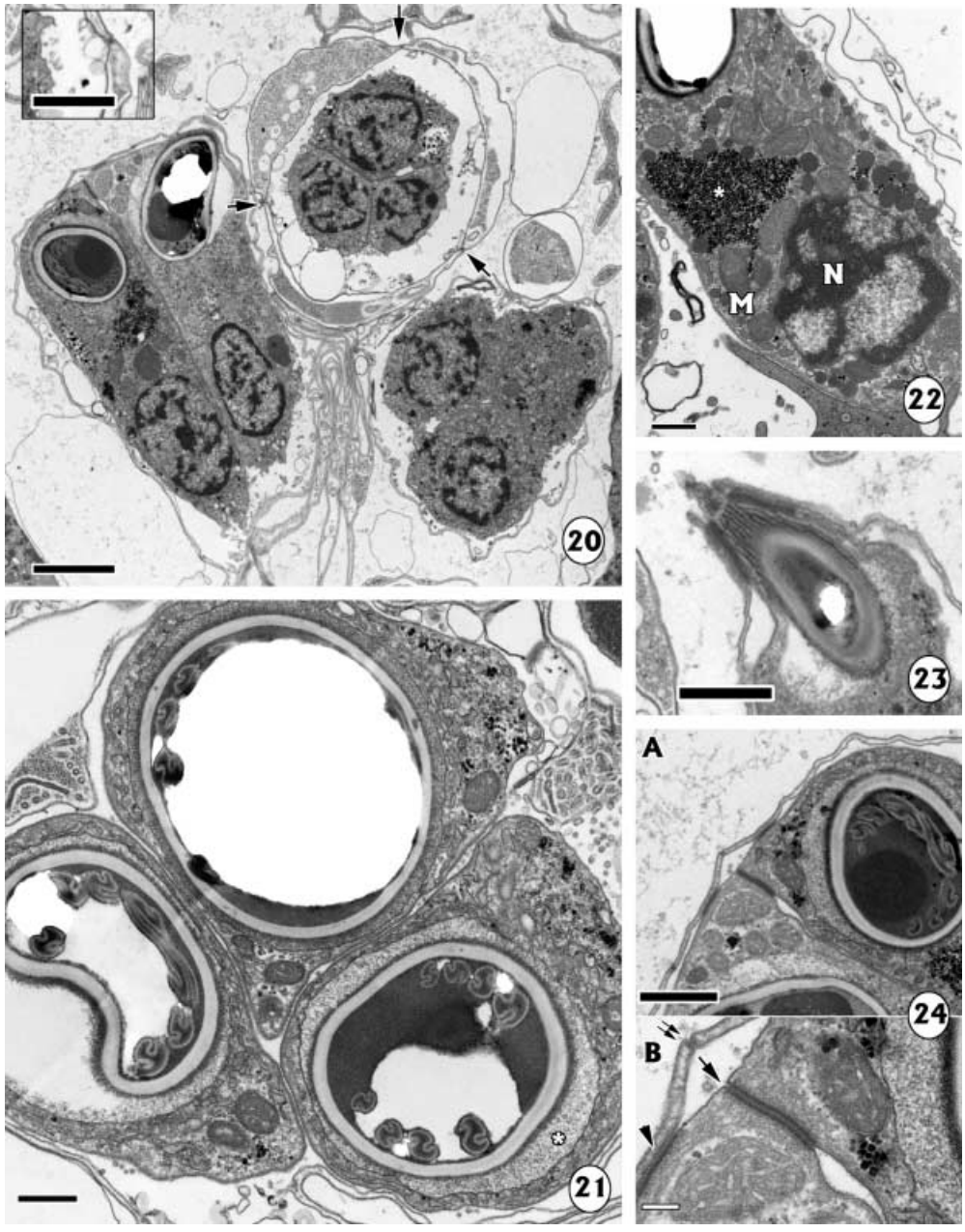

Figs. 20–24 Transmission electron micrographs of *Myxobolus pseudodispar* triactinospores in the tubificid host

Fig. 20 Pansporocyst harbouring spores sectioned at different levels of the capsulogenic cells. Notice the three capsulogenic cells in transverse section surrounded by the three valvogenic cells connected by junctions (*arrows* and *inset*). *Bar* 2 μm, *inset* 1 μm

Fig. 21 Cross-section of the three capsulogenic cells at the level of the polar capsules. Notice the foamy space surrounding the polar capsule wall delimited by a membrane (*). *Bar* 0.5 μm

Fig. 22 Detail of the posterior part of a capsulogenic cell showing the nucleus (*N*), abundant mitochondria (*M*) and glycogen granules (*). *Bar* 0.5 μm

Fig. 23 Detail of a polar capsule showing the longitudinal ribs of the wall and the plug in the apex. *Bar* 1 μm

Fig. 24 **A** Detail of the apical part of a spore showing two capsulogenic cells and two thin valves. *Bar* 1 μm. **B** Note the desmosome-like junctions between both capsulogenic cells (*arrows*), the hemidesmosome-like junctions between a capsulogenic cell and the inner membrane of a valve (*arrowhead*), and the simple junction between valves (*double arrow*). *Bar* 0.2 μm

cytoplasm with ribosomes, little endoplasmic reticulum and few glycogen granules.

Discussion

Ultrastructural studies of the intraoligochaete stages of the two *Myxobolus* species supported the light microscopic results previously obtained on these parasites (Székely et al. 1999; Eszterbauer et al. 2000) and also confirmed, in general, the findings of Lom and Dyková (1997), Lom et al. (1997) and El-Matbouli and Hoffmann (1998).

The valvogenic cells in the mature specimens of both species contained only traces of cytoplasm and the latter was detectable only in the segment of the spore body. In most parts of the spore, valvogenic cells appeared as membrane doublets composed of an electron-lucent layer between two electron-dense layers. Other electron microscopic findings demonstrated that the actinospores of *M. bramae* and *M. pseudodispar*, although both of the triactinomixon type, differ in several respects. The number of infective cells in the actinospore of *M. bramae* was high. Analysis of longitudinal and transversal sections using light microscopy provided an estimate of 32 infective cells per actinospore (Eszterbauer et al. 2000). In ultrathin sections, a high number of infective cells could also be seen. This was in contrast to the small number of large infective cells, probably not more than 8 (Székely et al. 1999), in the sporoplasm of *M. pseudodispar*. Moreover, the infective cells of both species were quite different in

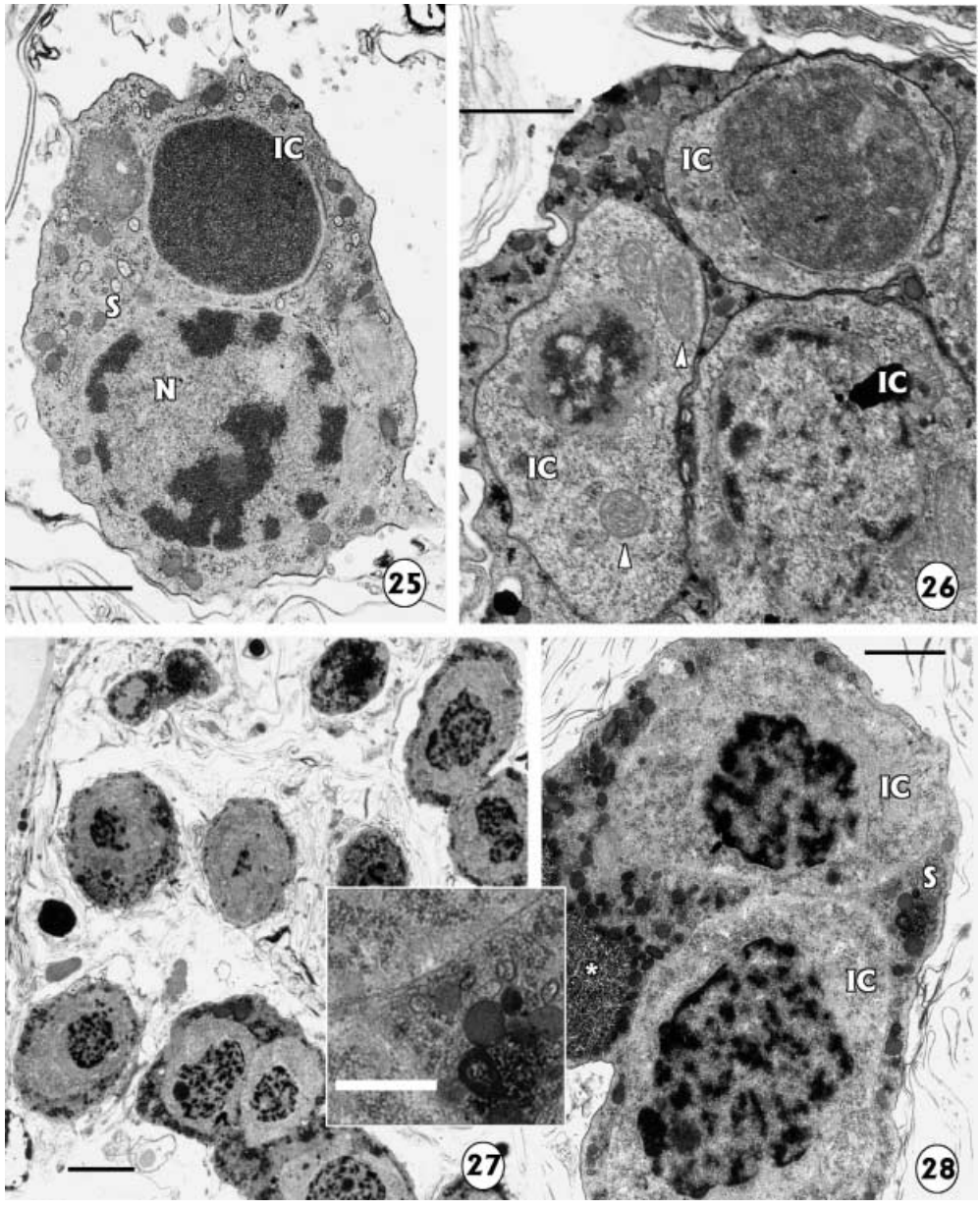

Figs. 25–28 Transmission electron micrographs of *Myxobolus pseudodispar* triactinospores in the tubificid host

Fig. 25 Sporoplasm (*S*) in initial steps of division showing a vegetative nucleus (*N*) and an initial infective cell (*IC*). *Bar* 1 μm

Fig. 26 Sporoplasm (*S*) in initial steps of division showing three *IC* in different maturation stages. Notice the large mitochondria in one vegetative cell (*arrowheads*). *Bar* 1 μm

Fig. 27 Panoramic view of a pansporocyst showing mature sporoplasms with infective cells, sectioned at different levels. *Bar* 2 μm

Fig. 28 Detail of a sporoplasm (*S*) with two infective cells (*IC*). Note the glycogen granules (*) and details of sporoplasmosomes and vesicles in S (*inset*). *Bar* 1 μm; *inset* 0.5 μm

appearance. There was a significant difference between the two species in the position of the capsulogenic cells in relation to the sporoplasm. In the case of *M. pseudodispar*, elongated capsulogenic cells were located anterior to the sporoplasm and well separated from it. The sporoplasm of the triactinospores of *M. bramae* was, however, clearly extruded among the capsulogenic cells. El-Matbouli and Hoffmann (1998) reported a similar situation in the triactinospore of *M. cerebralis*.

Although we only obtained a few data on the formation of the polar capsules, we can support the finding of Lom and Dyková (1997) that there is a special membrane-limited space between the wall of the polar capsule and the cytoplasm of the capsulogenic cell. However, whereas in *M. bramae* only a narrow lucent space without cell organelles was observed, in the case of *M. pseudodispar* this space seemed to be filled by a foamy cytoplasm. This could also be due to the different stage of maturation, which was more advanced in *M. bramae*, as suggested by Lom et al. (1997) for *Triactinomyxon*. The examination of the wall of the polar capsule in the actinospores of *M. bramae* and *M. pseudodispar* showed a series of ribs running longitudinally on its surface. This finding corresponds to the observations of Lom and Dyková (1997) and Lom et al. (1997), in the triactinomyxon stage of *M. cerebralis* and the raabeia stage of *Myxobolus cultus*.

Early developmental stages were mainly observed in *M. pseudodispar*, and they were, in general, coincident with equivalent stages described previously. The pregametic cells were similar to those described by Lom et al. (1997) for *Aurantiactinomyxon* and those described by El-Matbouli and Hoffmann (1998) for the triactinomyxon stage of *M. cerebralis*. The zig-zagging

cisternae of endoplasmic reticulum were also reported by Lom et al (1997), who considered them to be unique in the myxozoa. The existence of gametic stages was confirmed by the presence of polar bodies, indicating a previous meiosis as described by Marques (1986), though synaptonemal complexes were not clearly observed. The second meiotic division, as suggested by Marques (1986), probably occurred as well, as indicated by the presence of polar bodies in the more advanced stages (Fig. 15).

Different types of cell junctions were observed. The electron-dense junctions connecting the pansporocyst cells in *M. bramae* were considered similar to tight junctions as in *Sphaeractinomyxon ersei* (Hallett et al. 1998). However, Lom et al. (1997) described simple junctions between enveloping cells in both *Aurantiactinomyxon* and *Raabeia*, although these were considered to be more elaborate than the gap junctions between capsulogenic cells and between capsulogenic and valvogenic cells. Connections between the valvogenic cells of *M. pseudodispar* mature actinospores seemed to be simple adherent junctions and were not septate. Other actinosporea also showed no septate junctions between these cells (Lom and Dyková 1997), though septate junctions have also been reported (Lom and Dyková 1997). In our study, the most elaborate cell junctions were observed between the capsulogenic cells and between the valvogenic membrane and the capsulogenic cell of *M. pseudodispar*. The ultrastructural characteristics of these junctions are similar to those of desmosomes and hemidesmosomes, respectively. Nevertheless, the connections between these cell types have been reported as gap junctions by Lom et al. (1997) in both *Aurantiactinomyxon* and *Raabeia*. Further studies at the functional and biochemical levels are necessary to elucidate the real nature of the different junctions we have observed, and to confirm whether they are similar to the desmosomes, hemidesmosomes or other junctions of higher eukaryotes.

Acknowledgements The authors wish to acknowledge the CSIC – Hungarian Academy of Sciences Agreement for supporting this work. We are grateful to technicians from the Electron Microscope Service of the University of Barcelona for TEM processing. Additional financial help was provided by research grant MAR98/1000 from the Spanish CICYT and contracts T 029200 and T 031755 from the Hungarian Scientific Research Fund (OTKA). The authors also declare that all the experiments comply with the current laws of Hungary, where the experimental infections were performed.

References

De Puytorac P (1963) L'ultrastructure des cnidocystes de l'Actinomyxidie: *Sphaeractinomyxon amanieui* sp. nov. C R Acad Sci 256:1594–1596

El-Matbouli M, Hoffmann RW (1998) Light and electron microscopic studies on the chronological development of *Myxobolus cerebralis* to the actinosporean stage in *Tubifex tubifex*. Int J Parasitol 28:195–217

Eszterbauer E, Székely C, Molnár K, Baska F (2000) Development of *Myxobolus bramae* (Myxosporea: Myxobolidae) in an oligochaete alternate host, *Tubifex tubifex*. J Fish Dis 23:19–25

Grossheider G (1994) Untersuchungen zum Lebenszyklus von *Sphaerospora renicola* Dyková et Lom, 1982 und *Hoferellus cyprini* Berg, 1898 (Myxozoa: Myxosporea) aus der Niere des Karpfens *Cyprinus carpio* L. Thesis, University of Hannover, Germany

Hallett SL, O'Donoghue PJ, Lester RJG (1998) Structure and development of a marine actinosporean, *Sphaeractinomyxon ersei* n. sp. (Myxozoa). J Eukaryot Microbiol 45:142–150

Koller E (1994) Verbreitung von Actinosporea in zwei Salmoniden-Teichwirtschaften. Diploma tthesis, University of Munich, Germany

Lom J, Dyková I (1992) Fine structure of *Triactinomyxon* early stages and sporogony: myxosporean and actinosporean features compared. J Protozool 39:16–27

Lom J, Dyková I (1997) Ultrastructural features of the actinosporean phase of Myxosporea (Phylum Myxozoa): a comparative study. Acta Protozool 36:83–103

Lom J, Yokoyama H, Dyková I (1997) Comparative ultrastructure of *Aurantiactinomyxon* and *Raabeia,* actinosporean stages of myxozoan life cycles. Arch Protistenkd 148:173–189

Marques A (1982) Complexes synaptonémaux et stades initiaux ches les Actinomyxidies. C R Acad Sci 295:501–504

Marques A (1983) La fécondation et les premieres stades de la sporogénese d'une Actinomyxidie. C R Acad Sci 296:717–720

Marques A (1984) Contribution á la connaissance des Actinomyxidies. Ultrastructure, cycle biologique, systématique. Thesis, Université S. T. L. Montpellier, pp 219

Marques A (1986) La sexualité ches les Actinomyxidies: Etude chez *Neoactinomyxon eiseniellae* (Ormieres et Frésil, 1969), Actinosporea Noble, 1980: Myxozoa Grassé, 1970. Ann Sci Nat Zool 13e sér 8:81–101

Molnár K, El-Mansy A, Székely Cs, Baska F (1999) Experimental studies on the intraoligochaete development of myxosporean fish parasites (in Hungarian). Magy Allatorv Lapja 121:283–291

Ormieres R (1970) Formation des capsules polaires dans la spore de l'Actinomyxidie *Aurantiactinomyxon eiseniellae* Orm. Fré. (Étude ultrastructurale). C R Acad Sci 271:2326–2328

Reynolds ES (1963) The use of lead-citrate at high pH as an electron-opaque stain in electron microscopy. J Cell Biol 17:208–212

Spurr AR (1969) A low-viscosity epoxy-resin embedding medium for electron microscopy. J Ultrastruct Res 26:31–43

Székely C, Molnár K, Eszterbauer E, Baska F (1999) Experimental detection of the actinospores of *Myxobolus pseudodispar* (Myxosporea: Myxobolidae) in oligochaete alternate hosts. Dis Aquat Org 38:219–224

Wolf K, Markiw ME (1984) Biology contravenes taxonomy in the myxozoa: new discoveries show alternation of invertebrate and vertebrate hosts. Science 225:1449–1452

Yokoyama H, Ogawa K, Wakabayashi H (1991): A new collection method of actinosporeans – a probable infective stage of myxosporeans to fishes – from tubificids and experimental infection of goldfish with the actinosporean, *Raabeia* sp. Fish Pathol 28:135–138